Performance of a dense urban massive MIMO network from a simulated ray-based channel

Mohammed Zahid Aslam[1*], Yoann Corre[1], Emil Björnson[2] and Erik G. Larsson[2]

Abstract

Massive MIMO network deployments are expected to be a key feature of the upcoming 5G communication systems. Such networks are able to achieve a high level of channel quality and can simultaneously serve multiple users with the same resources. In this paper, realistic massive MIMO channels are evaluated both in single and multi-cell environments. The favorable propagation property is evaluated in the single-cell scenario and provides perspectives on the minimal criteria required to achieve such conditions. The dense multi-cell urban scenario provides a comparison between linear, planar, circular, and cylindrical arrays to evaluate a large-scale multi-cell massive MIMO network. The system-level performance is predicted using two different kinds of channel models. First, a ray-based deterministic tool is utilized in a real North American city environment. Second, an independent and identically distributed (i.i.d.) Rayleigh fading channel model is considered, as often used in previously published massive MIMO studies. The analysis is conducted in a 16-macro-cell network with both randomly distributed outdoor and indoor users. It is shown that the physical array properties like the shape and configuration have a large impact on the throughput statistics. Although the system-level performance with i.i.d. Rayleigh fading can be close to the deterministic prediction in some situations (e.g., with large linear arrays), significant differences are noticed when considering other types of arrays. The differences in the performance of the various arrays utilizing the exact same network parameters and the same number of total antenna elements provide insights into the selection of these physical parameters for upcoming 5G networks.

Keywords: Massive MIMO, Channel modeling, Ray-based model, Performance evaluation, 5G

1 Introduction

Massive MIMO (maMIMO) technology has been shown to provide the requirements set by the 5G standard in various studies and the literature. It helps to improve the spectral efficiency and utilize the available channel resources more efficiently. Although many operators and equipment manufacturers have today conducted controlled experiments to demonstrate the possible gains of this technology, large-scale deployments of the technology and its network-level performance in real scenarios is yet to be seen.

In this paper, a realistic ray-based propagation channel has been utilized to predict the performance of a dense urban maMIMO network with different settings. Such a study makes it possible to better understand and apply the technology in realistic environments, which can significantly differ from theoretical analysis. It also permits to properly anticipate the possible applications and gains, refine the systems, and prepare the deployment strategies. Single-cell analysis considering multiple simultaneous users [1, 2] in realistic environments only provides a partial perspective of the network performance. In this paper, a multi-cell network is deployed in a real and complex environment, which is precisely represented into 3D geographical data. A combination of both outdoor and indoor users is considered to best reflect realistic conditions, with indoor users distributed in different building floors. The obtained physical channels are then utilized to perform precise system-level simulations [3] leading to the assessment of the user throughput. The simulator implements state-of-the-art signal processing schemes, including transmit precoding and power allocation techniques. It supports multi-cell multi-user scenarios and

*Correspondence: zaslam@siradel.com
[1]SIRADEL, 2 Parc de Brocéliande, St. Grégoire, France
Full list of author information is available at the end of the article

computes inter- and intra-cell interferences. It can take any kind of MIMO channel data as an input, which made the interface with the ray-based channel model straightforward.

Similar to the current 4G macro base station (BS) sites, the maMIMO base stations are considered to be located on the rooftops of dominant buildings with roughly constant inter-site distance. In maMIMO systems, the number of antenna elements can be large as compared to the existing systems, and this permits the possibility of utilizing different antenna shapes like linear, planar, circular, and cylindrical arrays. Those different shapes are considered in this study to evaluate how the performance of the network changes while all other inputs are constant. The same approach can further be applied to different complex networks with varying inter-site distances (ISD), sectorization, and even complemented with a dense small-cell network, in order to determine the best deployment strategy for given objectives into a particular environment. These complex network changes are out of scope of the presented study. The paper also explores how the chosen channel model impacts the estimated maMIMO performance. The throughputs that have derived from the ray-based channel environments are drawn against those of a basic statistical model, as often used in the evaluation studies.

The large number of BS antennas of a maMIMO system allows for large spatial degrees of freedom to serve multiple users in the same time-frequency resource. It actually contributes towards two key maMIMO physical properties known as favorable propagation and channel hardening as described in [4] and [5], respectively. Together, these properties should enable a maMIMO system to spatially separate all the simultaneous users [2] (even if closely located) and provide stable stationary channel conditions, even with small user movements. These conditions are satisfied when very large arrays are considered. But in reality, the array size of a maMIMO system is limited, although large. Especially, when considering 3D arrays like cylindrical arrays, the aperture of the antenna array is limited as compared to a linear array. With these physical limitations, it is important to assess and demonstrate the performance of practical maMIMO systems in real propagation conditions.

The performance of the maMIMO system depends on the cross-correlation between channels, either the multiple channels from all array elements to a single user or the channels from one base station to the simultaneous users (that may cause mutual interference) [2]. For accurate predictions, this requires the channel models to be spatially consistent, i.e., to be able to reproduce variations and correlations between two antenna positions. Independent and identically distributed (i.i.d.) channel models do not support such spatial correlation and can therefore not accurately predict maMIMO channels. Some other models like geometry-based stochastic channel models (GSCM) create spatially correlated channels, thus might be appropriate; however, they are not able to manage the specificities of a particular physical environment [2]. The ray-based deterministic channels also provide inherent correlation, due to the computation of the physical wave propagation and interactions, but have the additional advantage that they can be run in real environments, using geographical map data. Therefore, they are relevant to assess various kinds of network topologies in a very accurate manner.

Section 2 describes briefly the system-level maMIMO simulator and its usage to obtain the rates that are achievable by the maMIMO system. Section 3 details the single-cell and multi-cell multi-user scenarios and setup, located in a North American dense urban area. Section 4 studies the multi-cell maMIMO channel characteristics. Section 5 presents the evaluation of the single-cell study with regard to favorable propagation. Section 6 discusses the system-level maMIMO performance for different antenna array shapes and configurations along with different channel models. Finally, Section 7 provides some conclusions, perspectives, and future work to be conducted on maMIMO system-level studies, with 5G radio planning as an objective.

2 Massive MIMO system-level simulator

The first open-source system-level simulator for maMIMO systems was delivered as supplementary material to the book [3]. This MATLAB simulator supports the state-of-the-art methods for channel estimation, receive combining, transmit precoding, and power allocation, as well as quantifying the corresponding achievable rates. While some of these methods are tailored for statistical channel models, with known first- and second-order moments, in this paper, we use methods that support any channel model. More precisely, we consider least-square channel estimation (under the presence of pilot contamination) and regularized zero-forcing (RZF) precoding. The power allocation is selected to maximize the product of the users' effective SINRs, which is essentially the same as maximizing the sum rate, except that there is a "bias" towards giving higher rates to the most unfortunate users than they would get with pure sum-rate maximization (which could lead to zero rate for the weakest users). The rates presented in this paper are obtained for full-buffer transmission. We have modified the original simulator from [3] to support our setup, for example, by including BS user association.

In a maMIMO system, the number of simultaneous users is typically much smaller than the number of BS antennas, because there is a limited number of pilot sequences available for channel estimation. In this paper,

we have considered a maximum of 20 active users that can be connected to any single BS simultaneously. If there are more users, then the system has the possibility to select and allocate some of them on different time slots or frequency sub-bands (maMIMO scheduling). Once a set of users is selected for simultaneous allocation, i.e., at the same time and frequency, the BS allocates 1 of the 20 pilots uniformly at random to the users. Each pilot is only used once per cell, but will be reused across cells, which leads to pilot contamination. The different propagation and interference conditions experienced by the users are partly mitigated by carefully attributing the powers.

3 Simulation methodology and scenario

To evaluate the performance of a maMIMO system, two different scenarios have been considered. A single-cell multiple simultaneous user environment is first evaluated for the minimum conditions similar to favorable propagation (FP) that can be achieved. Then, a multi-cell network of maMIMO macro BS is considered to evaluate the performance of the network considering signal processing schemes for different antenna array shapes. The first scenario provides insights into the minimum horizontal separation required for a maMIMO BS to be successfully able to differentiate between users. Whereas, the second scenario evaluates these results in a large-scale realistic maMIMO environment with 3D spatial distributions of the users.

The selected scenarios utilizes 3D geographic map data from New York City, which includes buildings of varying heights. The selected area contains various different geographic features like narrow and wide streets, open squares, and cross sections. This map data makes it possible to obtain realistic and highly variable channel predictions for the considered scenarios.

To evaluate the favorable propagation conditions, three different sites as shown in Fig. 1, are selected. At each site, two simultaneous users are considered to be located in close proximity to each other. In Fig. 2, a depiction of the gradually increasing linear distance between the users is shown. The deterministic channels are then extracted from the ray-tracing tool for these user positions in close proximity. These channels are then evaluated for the level of favorable propagation in Section 5.

Further, to analyze the network-level performance, a network of macro-cell maMIMO BSs is considered. The carrier frequency is 3.5 GHz. All the BSs are equipped with directional antenna elements with a horizontal half power beamwidth (HPBW) of 90°, and a vertical HPBW of 20°, except in the results of Fig. 14 where this element is compared with another having a vertical HPBW of 60°. All the antennas are vertically polarized with a maximum gain of 13.3 dBi. The 3D beam pattern of the antenna
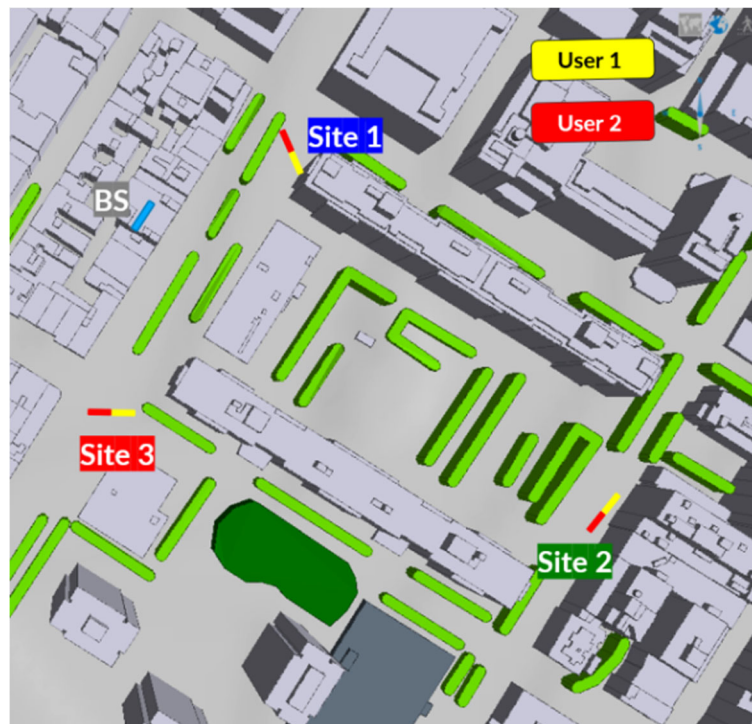
Fig. 1 Single-cell macro base station scenario
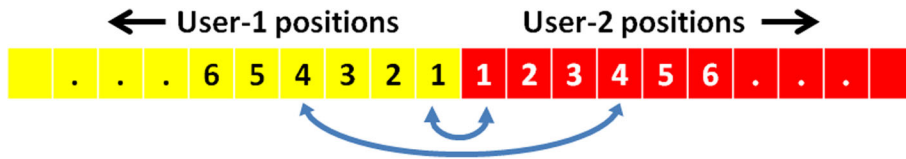
Fig. 2 Illustration of the separation of the simultaneous users in the single-cell macro base station scenario
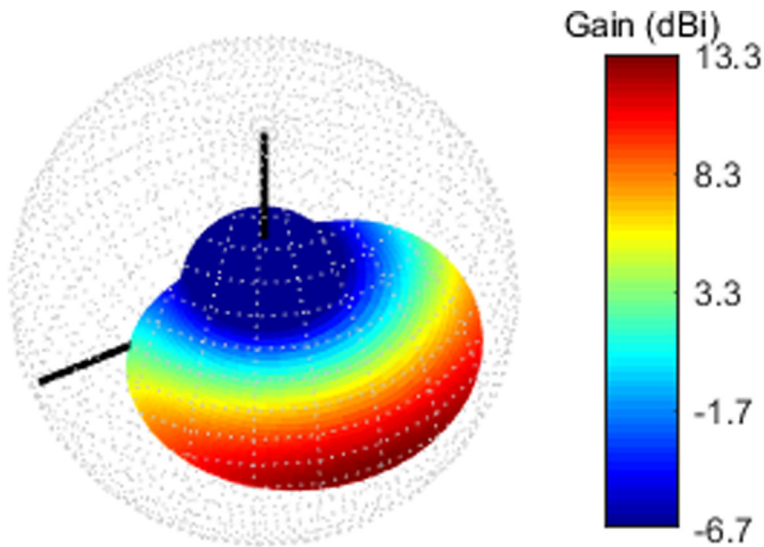
Fig. 3 Directional antenna array pattern of each antenna element in the maMIMO array

Fig. 4 Massive MIMO BS deployment area. The BSs are depicted by blue dots. The study area is 1.35 km^2. The different colors in the streets represent the color corresponding to their best serving BS for that area

used is shown in Fig. 3. The total transmit power before the application of maMIMO power allocation schemes is 43 dBm over a 20-MHz bandwidth. The network is composed of 16 maMIMO BSs located on top of dominant (or quasi dominant) buildings such that the area of interest shown in Fig. 4 is fully covered. Each BS array is formed of 192 antennas. The average inter-site distance (ISD) is 320 m over an area of 1.6 km^2. The furthest BSs (diagonally opposite) are located 1.365 km apart. The user equipment (UE) consists of a single omni-directional antenna with vertical polarization, located 1.5 m above the ground/floor level. Both indoor users located at multiple floors and outdoor users are simultaneously considered.

The objective of evaluating the network-level performance of a maMIMO system in real environments is to predict the maMIMO gains as accurately as possible. Such an approach also enables the comparison of physical parameters like different antenna shapes and their corresponding performance in the same network. Results in [1] and [6] suggest that the rate performance in many real propagation environments is comparable to the i.i.d. Rayleigh fading. Some explanations of the reason for this is given in [4]. This is due to the favorable propagation and channel hardening properties of maMIMO, which appear as the number of antennas at the BS increase. In reality, the number of BS antennas are limited (far from infinity) and deployed in a limited amount of space, depending on the antenna configuration. This limits the ability of large antenna arrays to observe various channel components.

This is demonstrated in this work by comparing several antenna sizes containing the same number of elements using a ray-based deterministic model.

4 Multi-cell massive MIMO channel characterization

The complex propagation environment creates rich multi-path components, which are predicted by the physical volcano urban ray-based model [7]. These multi-paths affect the maMIMO performance, either by creating spatial separability of users located close to each other or, on the contrary, by producing cross-correlation between users reached by the same canyoning or diffracting phenomenon. The use of a physical channel model does intrinsically bring all correlation factors, between cells and users, which are required for accurate maMIMO assessment.

In Fig. 5, an example of two different users connected to the same BS is shown. It can be seen that the propagation paths to user 1 are significantly different to those to user 2. Since user 1 is located in an open square, the propagation environment is well spread out and multiple strong propagation paths are available to the user; this would constitute a strong channel. In case of user 2, however, the propagation environment is limited due to the narrow street, and multiple strong propagation paths are not possible to be connected to this user. Both these users can be simultaneously served by the same BS since the channels are very different, and the BS must optimize its available resources to provide the best performance. This
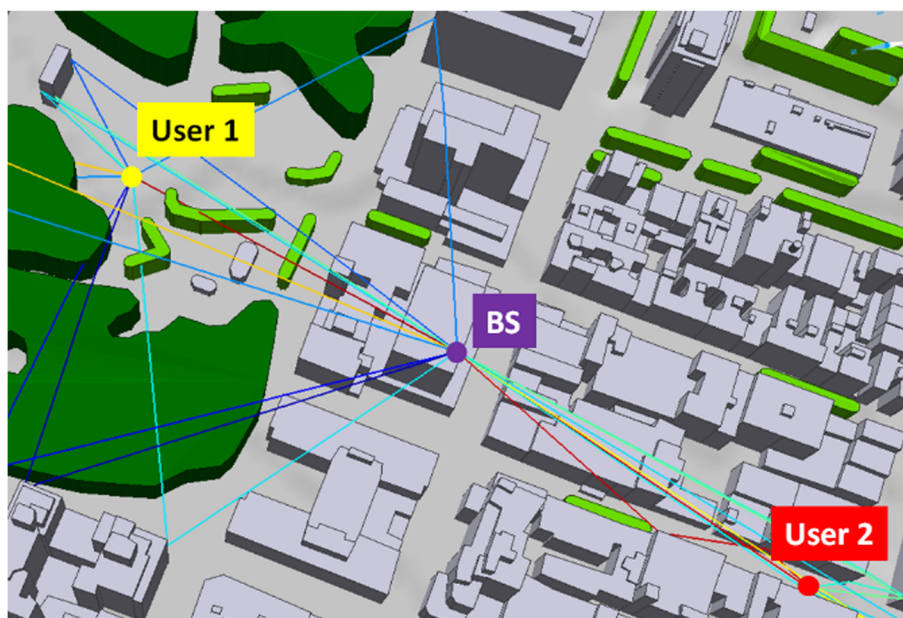
Fig. 5 Example of two users connected to the same BS having very different propagation paths
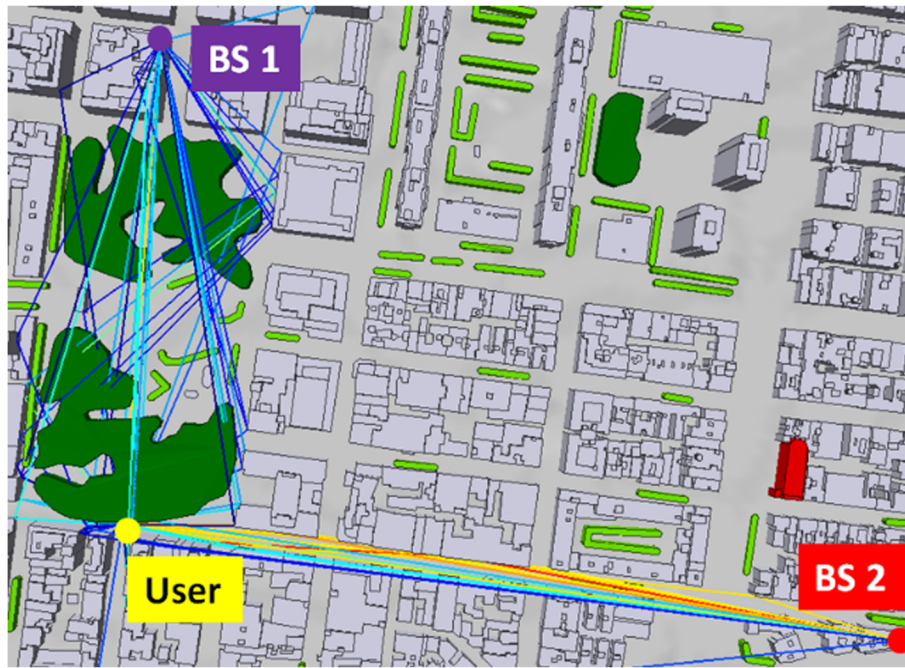
Fig. 6 Example of single user connected to multiple BSs by different propagation paths (canyoning/open square)

is achieved by jointly selecting the precoding and power allocation at the BS. In this paper, the maximum product SINR power allocation scheme is used along with the RZF transmit precoder.

In Fig. 6, an example of a single user with connections to two different BSs is shown. The user location is chosen such that the different propagation environments can be demonstrated. The propagation paths to the user from BS-1 in the large square contain multiple strong line-of-sight (LoS) and reflected paths. From BS-2, strong propagation paths are limited due to the urban canyon effect in the narrow street that reduces the signal power significantly due to multiple reflections. In such cases, the serving BS must be selected such that it provides the best received power to the user, even if another BS is physically located closer. This is known as the best server selection and is used in this paper. Figure 4 shows the best server selection by different colors in the streets, which correspond to a particular BS. To maximize the rates, the users are always connected to the BS that provides the best channels to them rather than the BS that is the closest to the user.

The channel model produces multi-paths from reflections and diffractions on the building facade, as well as rooftop diffraction. Channel properties, in particular, the departure angles, are depending on the specific physical situation of each BS-user link. The channel properties are predicted from an antenna element at the center of the BS array and then extrapolated to the whole array,

by assuming the multi-paths are stationary (i.e., persistent along with constant amplitude).

In Fig. 7, an illustration of the maMIMO BS connected to a random selection of simultaneous users located at different horizontal and vertical locations in the New York City map data is shown. The indoor users are located at different floors of multiple buildings of varying heights, and user-2 is an outdoor user on the street level. Although the users are located at different heights, from the macro BS location, a larger horizontal spread can be observed as compared to the vertical spread. The impact of this is explained in the results provided in Section 6.

5 Results and discussions from favorable propagation simulations

In Figs. 8 and 9, Eq. (1) [2] has been used to evaluate the favorable propagation in the deterministic channels obtained from the three different sites from Fig. 9.

$$\text{FPmetric} = \frac{\left| h_i^H h_k \right|^2}{\|h_i\|^2 \|h_k\|^2} \tag{1}$$

Here, h_i and h_k represent the different channel vectors obtained from the two simultaneous closely spaced users. The FPmetric verifies the correlation between the channels of the two closely spaced users such that a lower value of the FPmetric relates to better FP-like conditions. Further details on the equation and favorable propagation can be found in [2–4].
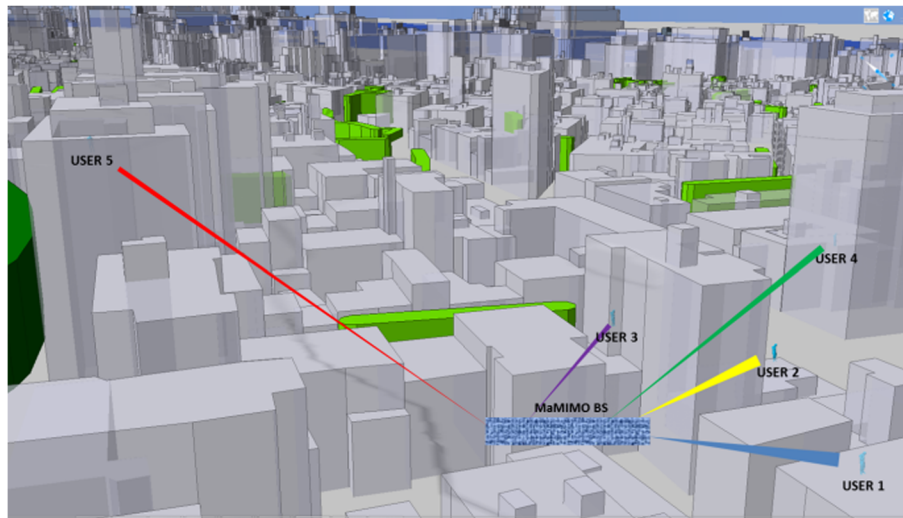
Fig. 7 Illustration of the outdoor and indoor user distribution on multiple floors of a typical North American city

When the geometric distance between the two users is considered, the propagation channels cannot be distinguished until a distance of 20 wavelengths (corresponding to 3 m for a frequency of 2 GHz). For the given scenarios, as the minimum distance between the two users increases to 20 wavelengths, FP-like conditions can be observed.

The distance between the BS and the user is also important to be able to differentiate the user channels, as observed from the BS. Two simultaneous users at different distances from the BS may experience different FP-like conditions. For this, the angle between the two users as observed from the BS provides a better perspective of the FP-like conditions. In Fig. 1, the users located at site 2 achieve FP-like conditions at the smallest angle. This is due to the distance between the BS and the users which is the largest in this location. In all three locations, FP-like conditions are achieved for an angular separation of 2.5°, between the users.
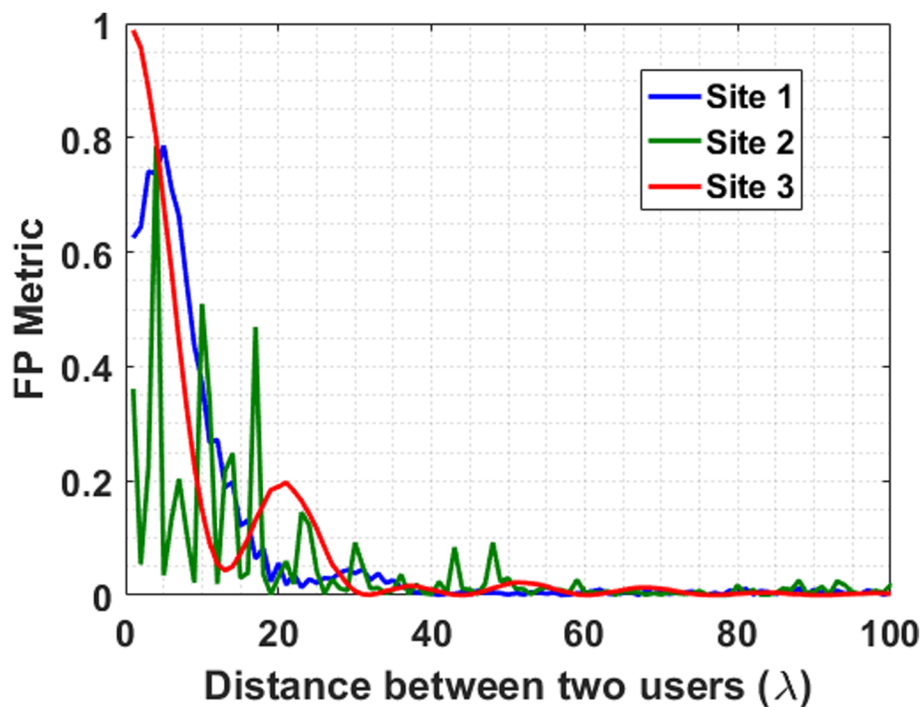
Fig. 8 Minimum distance required between the two users to obtain FP-like conditions
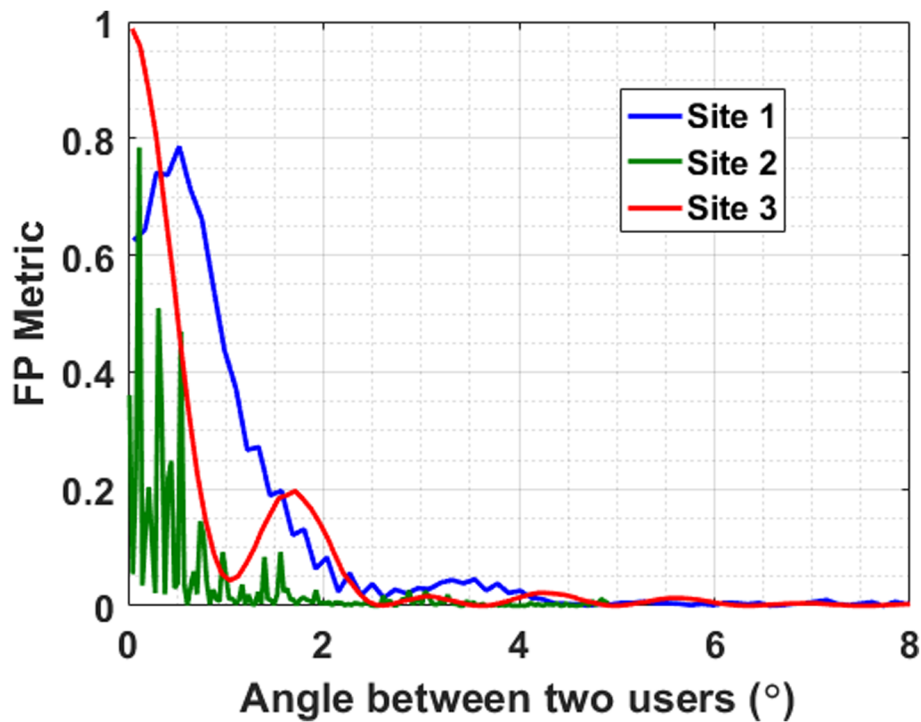
Fig. 9 Minimum angle required between the two users to obtain FP-like conditions

6 Results and discussions from massive MIMO multi-cell simulations

The performance statistics are obtained from a Monte-Carlo procedure. For the area covered by the 16 cells, 150 users are randomly dropped at each iteration. These user positions are a subset of 320 random user positions that are uniformly distributed in the entire computation area. The maMIMO propagation from all BSs to all 320 user positions are pre-computed. Then, each iteration is conducted in two successive steps; first, the maMIMO channel matrices are created for all BS-user combinations (based on pre-computed data); then, the system-level simulation is run as described in Section 2, including cell selection, precoding, power allocation optimization, and computation of achievable rates.
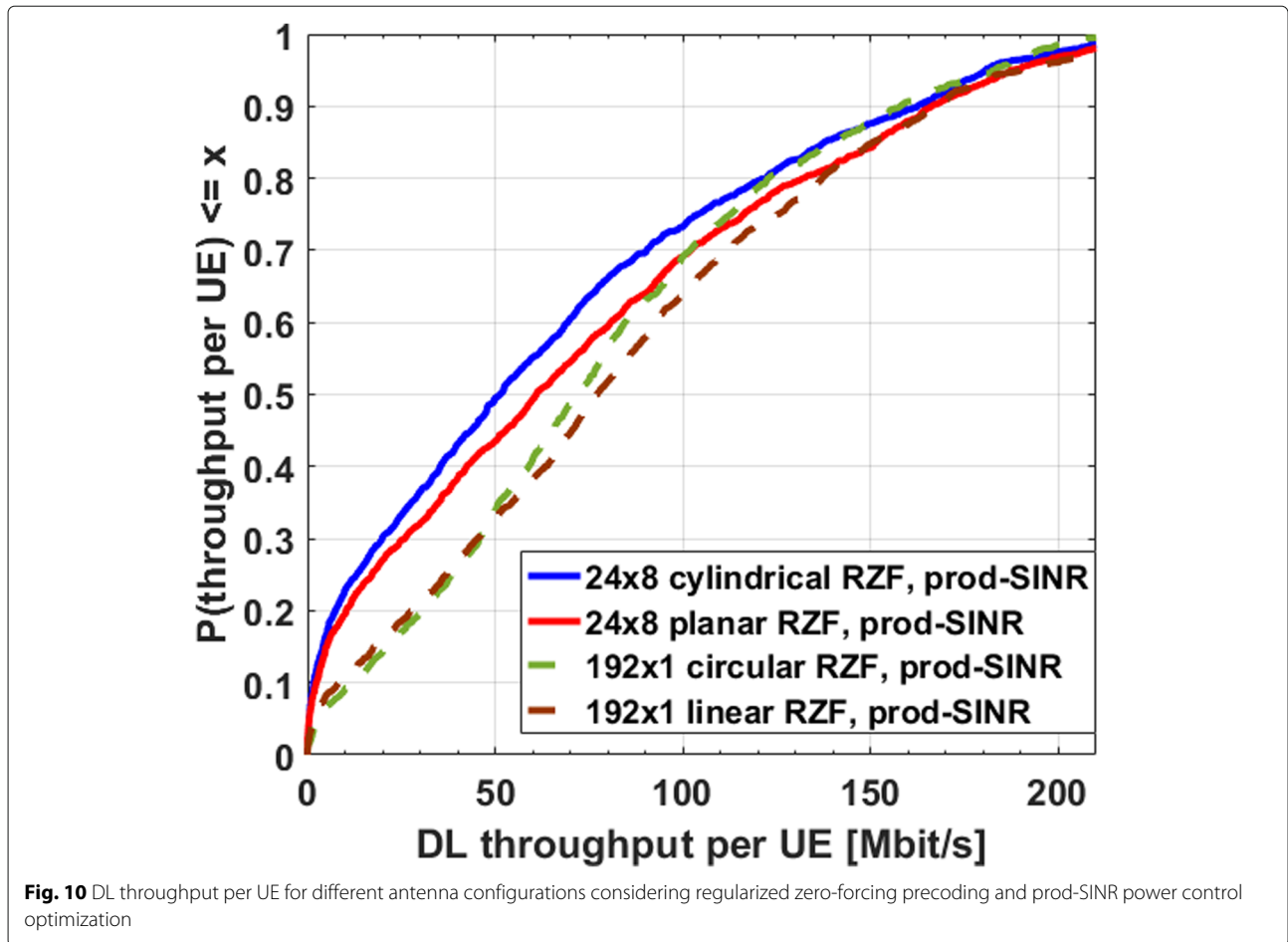
The system-level simulator presented in [3] is applied to the multi-cell maMIMO scenario described in Section 2. The channel data is obtained either from the statistical model (i.i.d. Rayleigh) or from importing the channel realizations created by the ray-based model. Several antenna array configurations are implemented and tested: linear, planar, circular, and cylindrical. Communication-theoretic data rate expressions given in [3] are used to evaluate the maMIMO performance.

All the considered arrays are uniform, and the adjacent antenna elements are separated by half wavelength. The linear array is a single row of 192 antenna elements

that are all directed in the same direction. It is more than 8 m long at 3.5 GHz. Due to this size, the practical installation of a 3.5-GHz linear array is unlikely, but this configuration is a particular case for which it is important to assess and compare the performance; that is why it is included in our study. The circular array is a single circular row of 192 antennas that face outwards from the circle with different but uniform orientations around the circle. Its physical diameter is 2.6 m, which remains quite large even for a macro base station. The planar array consists of 24 antenna elements in each of the 8 rows for a total of 192 antenna elements. Its dimensions are obviously reasonable for a practical deployment, with a length of 1 m and a height of 0.34 m. The cylindrical array is obtained similarly by considering a 24 × 8 setup with circular shape. The cylindrical antenna has the smallest dimensions among all the considered antennas; its diameter is less than 0.3 m. It is interesting to note that although the physical number of antenna elements is the same for the different array shapes, the dimensions can vary. These changes can significantly impact the performance of the network and have to be considered for accurate evaluations.

In Fig. 10, the cumulative distributive function (CDF) of the downlink (DL) throughput/rate per UE [3] is given for different antenna array configurations. In each simulation, outdoor users are randomly dropped in the considered

Fig. 10 DL throughput per UE for different antenna configurations considering regularized zero-forcing precoding and prod-SINR power control optimization

area. At the median percentile, the linear array performs the best with a throughput per UE of 76 Mbit/s. The cylindrical array performs the worst with a throughput per UE of 52 Mbit/s. This difference can be explained by the spatial aperture of each antenna array. The cylindrical array containing 192 antennas (24×8) has the smallest radius (dimension) of all the selected configurations. This is followed by the planar, circular, and linear arrays, which have similar median performance. At the highest percentiles, however, the performance of all different array configurations converges when the users all have good/favorable channel conditions in the outdoor scenario.

In Fig. 11, the i.i.d. Rayleigh fading channel is considered with the same multi-cell system-level simulator from [3]. The channel is defined only by the number of antenna elements for each user position and no correlation along the antenna coefficients or between user positions are considered. This model has the advantage of being easily implemented and analyzed, since there are closed-form rate expressions available in the literature [3], but the accuracy of the results is limited. In order to fairly compare the i.i.d. Rayleigh fading results with the deterministic setup, the path losses obtained from the deterministic setup are

also used in the i.i.d. Rayleigh fading setup. This process makes sure that the path losses between the two different channel models are the same, and therefore, we are able to compare the impact of the two channel models in terms of angular diversity and cross-link correlation. It can be seen from Fig. 11 that the performance of the normalized i.i.d. Rayleigh channel is similar to that of the deterministic channel in case of the linear array. At the median percentile, both the i.i.d. Rayleigh fading channel and the deterministic channel give a throughput of 80 Mbit/s per UE. However, if we consider the planar array, a significant loss in throughput can be observed. When considering the deterministic model, a DL throughput/rate per UE of 60 Mbit/s is obtained at the median value for the planar array. This difference of 20 Mbit/s between the planar and linear arrays is not seen in the i.i.d. Rayleigh model. The difference that is not captured by the i.i.d. Rayleigh model is due to the smaller aperture in the horizontal direction of the planar array.

For the sake of a comprehensible comparison, we were able to set the path losses in both deterministic and i.i.d. Rayleigh models to be the same. However, in reality, if we only consider i.i.d. Rayleigh fading channels, we normally
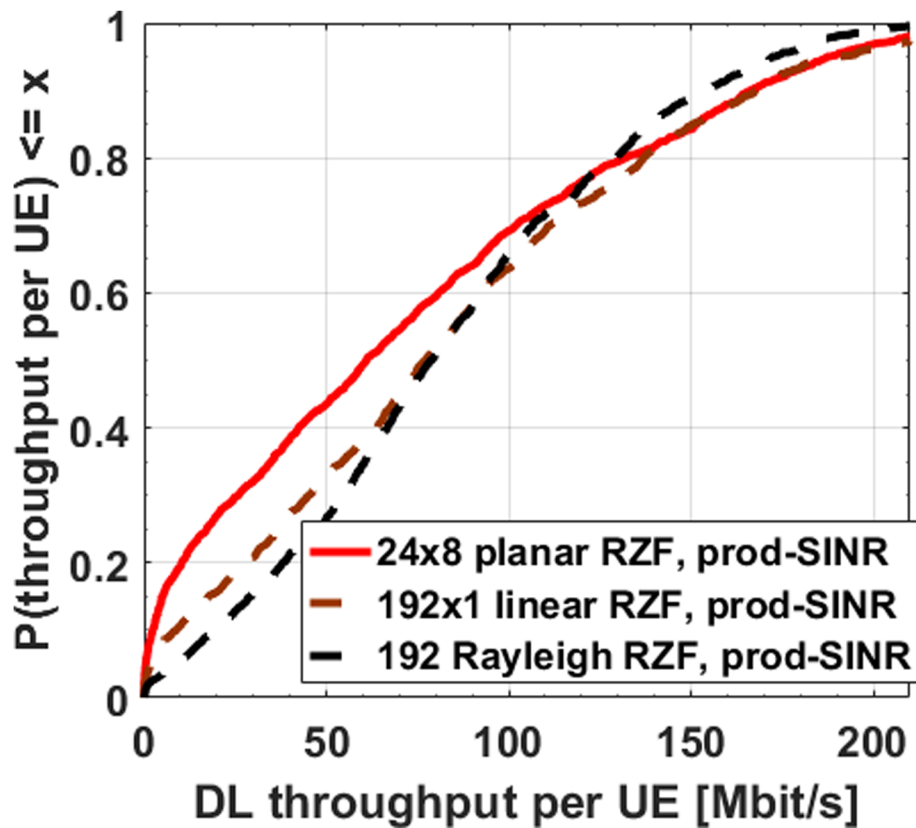
Fig. 11 DL throughput per UE for comparison of ray-based deterministic channel and i.i.d. Rayleigh based channel as applied to system-level simulations

do not have access to accurate models and the path loss information is obtained from more simple approaches (empirical models) which has to be chosen very carefully as small variations in the selection of the model can lead to very different results.
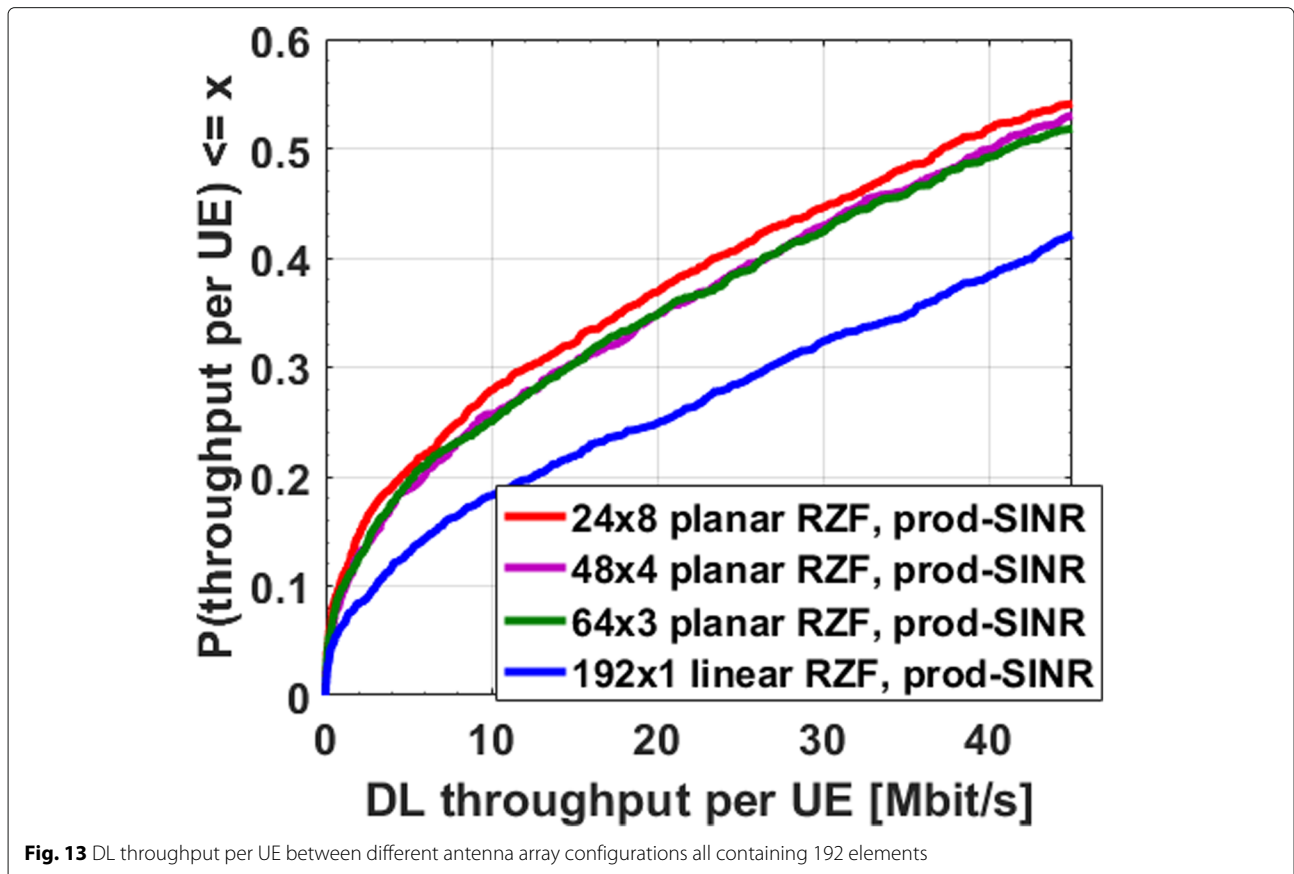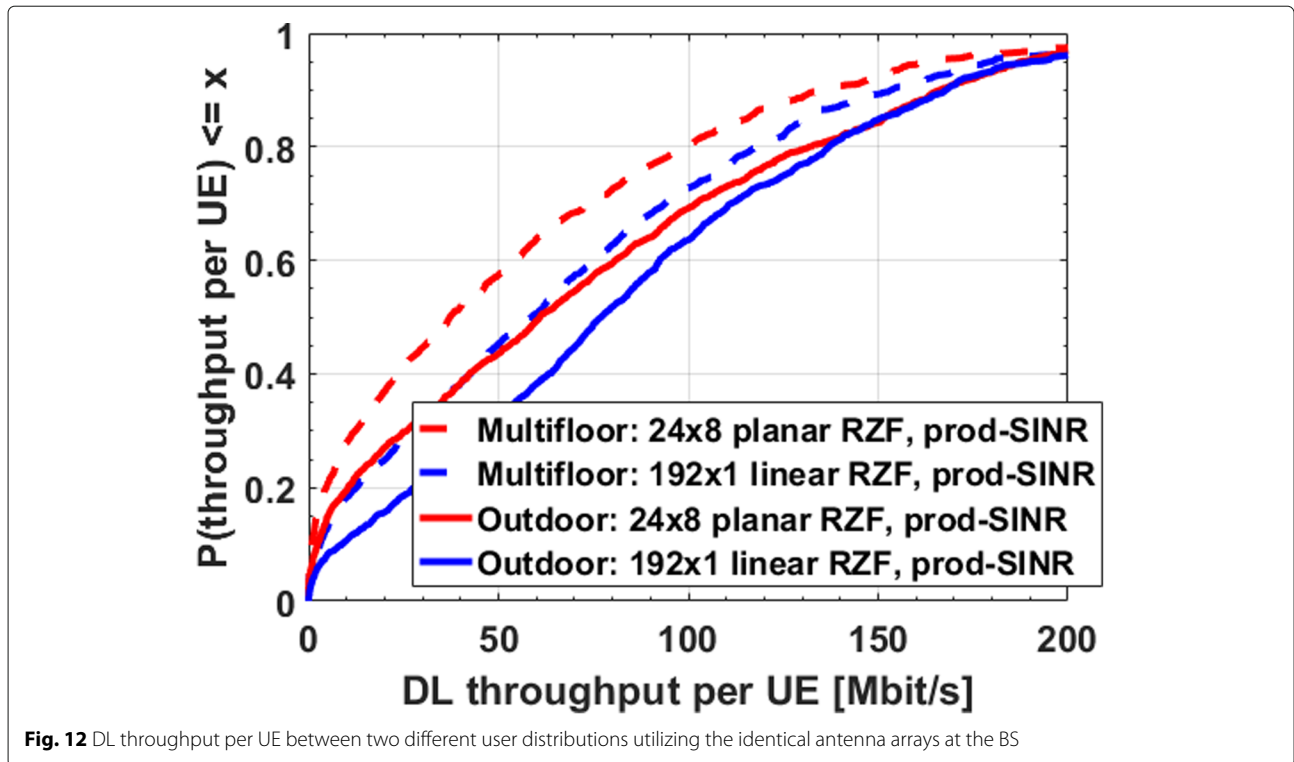
The largest throughput per UE utilizing the deterministic channels corresponds to the linear array followed by the arrays with the largest horizontal dimension. This can be explained as all the users considered are distributed in the horizontal plane (only located outdoors) and the vertical angle of the propagation paths does not vary much from one user to another. Therefore, the BS is mainly required to serve users by separating them in the horizontal direction. The addition of vertical antenna elements then does not contribute as much to the throughput.

In the last stage of our study, we considered a 3D user distribution, with 75% indoor users located at a random floor inside the buildings. The varying building heights are properly considered, so the highest buildings have more users, being uniformly distributed from the ground to the top floor. Due to the height dimension, even two users located at the same 2D location can be separated, as the minimum distance between two floors (3 m) could be sufficient to separate the users. This provides an

additional degree of freedom to the BS to separate closely spaced users and provide higher throughput.

This new scenario, where only the ray-based model is involved, investigates how the insertion of the vertical dimension in the user distribution affects the estimated maMIMO performance.

Both user distributions (outdoor only, or mixed) are considered in Fig. 12. The linear antenna array performs the best in both the user distributions as compared to the planar array. Although the indoor users provide better separability to the BS, the attenuation caused due to the outdoor-to-indoor propagation loss results in lower values of the data throughput. The linear array performance is expected to be better in the outdoor scenario as discussed in relation to Fig. 10; however, similar performance is noticed in the scenario with indoor users as well. This is due to the fact that the horizontal dimension is significantly dominant as compared to the vertical dimension, even when multi-floor users are simulated. At each simultaneous time-frequency slot, each BS is connected to a maximum of ten users. These users are located at different locations of the macro-cell, and although they are located at different heights, the horizontal spread of the users is greater. Indeed, if all the simultaneous users are located

Fig. 12 DL throughput per UE between two different user distributions utilizing the identical antenna arrays at the BS

Fig. 13 DL throughput per UE between different antenna array configurations all containing 192 elements

in the same building, this could be different. As shown in Section 5, the minimum distance or angle between two closely spaced users can be significantly small to achieve FP-like conditions, and the minimum separation of 3 m between different floors of a building may be sufficient to separate users in the vertical direction. Therefore, the worst case scenario would be when all the users are located in the same building present at the cell edge. However, since the probability of such an event is very small, we can conclude that the horizontal dimension still retains the significant role in macro-cell scenarios.

In Fig. 13, the impact of decreasing the horizontal dimension of the antenna array while maintaining the same number of total antenna elements is illustrated. Clearly, the linear array performs significantly better than the planar arrays due to its large horizontal aperture. The planar array with the smallest horizontal aperture with 24 horizontal elements has the lowest throughput performance with the other intermediate arrays in between. However, this does not mean that there is no impact of the vertical dimension and it must also be considered. In Fig. 14, 2 different types of individual antenna elements used in the arrays have been compared. The first element is the same as used in the rest of the study with a beamwidth of 90° in the horizontal direction and 20° in the

vertical direction. The second element has a larger vertical beamwidth of 60° and the same horizontal beamwidth. At the 40th percentile, when all the elements of the planar array are considered with the larger vertical beamwidth, a throughput of 20.5 Mbit/s is achieved whereas the smaller vertical beamwidth provides a throughput of 24 Mbit/s. It is interesting to note that the signal processing provides digital beamforming as well, and the impact of the antenna element beamwidth is limited. However, these results provide an insight into the careful selection of the physical parameters of the antenna arrays to provide the best possible performance. Such information about the physical parameters of the antenna arrays can also be useful in designing future hybrid antenna arrays that utilize fewer radio-frequency chains as well.

7 Conclusions

Practical maMIMO systems will have a large but limited number of antennas, which corresponds to limited spatial degrees of freedom and dimensions for the antenna array. The performance of the maMIMO system at the cell and system levels depends on the array structure but also on the propagation characteristics. This paper explored a mechanism to evaluate the favorable propagation conditions in a maMIMO channel utilizing
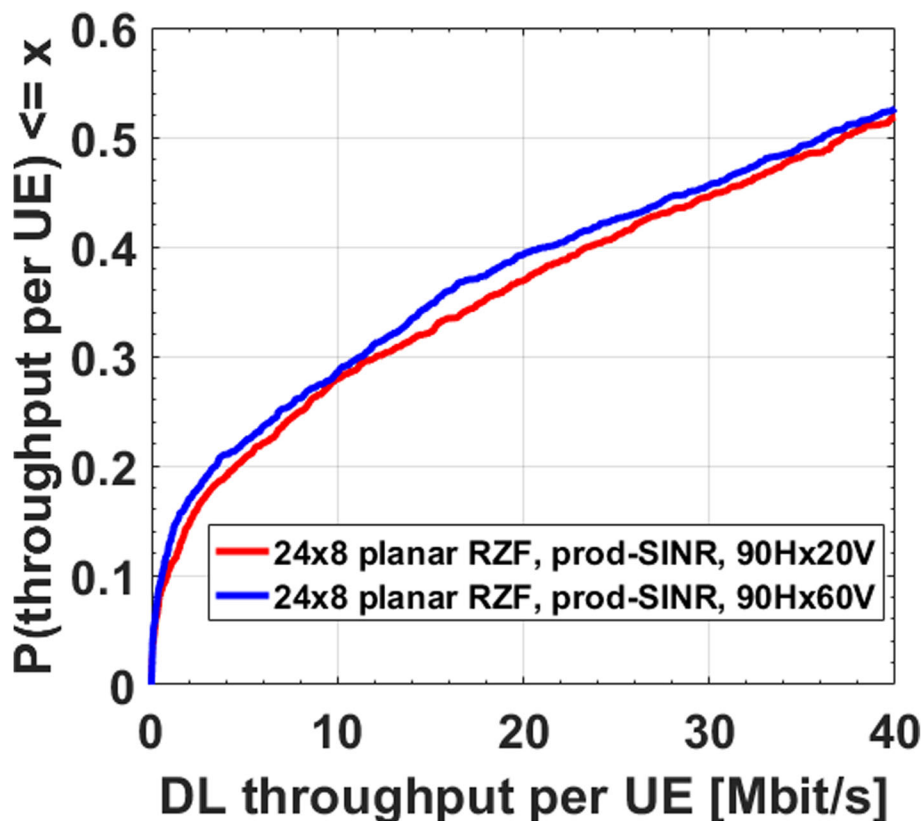
Fig. 14 DL throughput per UE between two different antenna elements with different physical vertical beamwidth

deterministic ray-based channels along with new simulation procedures to reach accurate prediction of a maMIMO network considering highly realistic user distributions in real environments.

The maMIMO channel responses from a ray-based deterministic tool were obtained and used for system-level simulations that include precoding and multi-user power allocation. A multi-cell macro deployment of 16 maMIMO BSs in a dense urban environment was evaluated. At the median percentile, the antenna array with the largest spatial aperture (linear) has the best performance as compared with the cylindrical array (smallest extent) which has the worst performance.

It is shown that at i.i.d. Rayleigh fading channels whose path losses have been set to the same values as those considered in the deterministic model provide rather similar throughput as the deterministic channel when considering the linear array. This can be explained by the fact that the large size of the linear array is able to see various different channel components that is closer to the uncorrelated channels represented by the i.i.d. channels. In the case of the planar array, the impact due to the limited horizontal dimension of the array is not captured by the i.i.d. Rayleigh model and leads to significantly different results.

Finally, the performance of a realistic maMIMO network considering 3D user distributions was provided. The performance of the maMIMO network for different configurations considering the layout of antenna array and also for different physical antenna patterns is provided. The results show that even when considering users located vertically on different floors, the linear array with large horizontal aperture performs better than the planar array. The reason for such performance is due to the physical locations of the simultaneous users in macrocells. Even when located at different heights, the number of simultaneous users is larger in the horizontal direction as compared to the vertical direction. Indeed, this could be different when considering small cells or a BS providing access to a fixed group of users like in a single large building. All the network parameters for these different results remain identical however just based on the selection of the antenna shape, layout of the array, and even the type of the beam pattern; differences can be observed in the overall performance of the network. A very large antenna array consisting of 192 elements has been considered, and these differences are expected to be larger when considering arrays with smaller dimensions. During the deployments of real maMIMO networks, such physical parameters must also be considered along with optimal signal processing schemes to obtain the best possible network performance. Another perspective of this work is also to predict deterministic maMIMO performance heatmaps, as will be required in 5G radio planning.

Author details
[1]SIRADEL, 2 Parc de Brocéliande, St. Grégoire, France. [2]Linköping University, 58183 Linköping, Sweden.

References
1. X. Gao, O. Edfors, F. Tufvesson, E. G. Larsson, Massive MIMO in real propagation environments: do all antennas contribute equally?. IEEE Trans. Commun. **63**, 3917–3928 (2015)
2. M. Z. Aslam, Y. Corre, E. Björnson, Y. Lostanlen, Massive MIMO Channel Performance Analysis Considering Separation of Simultaneous Users. Paper presented at the 22nd International ITG Workshop on Smart Antennas - WSA 2018, Bochum, Germany, 14-16 March 2018 (2018)
3. E. Björnson, J. Hoydis, L. Sanguinetti, Massive MIMO networks: spectral, energy, and hardware efficiency. Found. Trends Signal Process. **48**(11), 158–335 (2017)
4. H. Q. Ngo, E. G. Larsson, T. L. Marzetta, Aspects of favorable propagation in massive MIMO. Paper presented in 2014 Proceedings of the 22nd European Signal Processing Conference (EUSIPCO), Sept 2014, 76–80
5. B. M. Hochwald, T. L. Marzetta, V. Tarokh, Multiple antenna channel hardening and its implications for rate feedback and scheduling. IEEE Trans. Inf. Theory. **50**(9), 1893–1909 (2014)
6. X. Gao, O. Edfors, F. Rusek, F. Tufvesson, Massive MIMO performance evaluation based on measured propagation data. IEEE Trans. Wirel. Commun. **14**(7), 3899–3911 (2015)
7. Y. Corre, Y. Lostanlen, Three-dimensional urban EM wave propagation model for radio network planning and optimization over large areas. IEEE Trans. Veh. Technol. **58**(7), 3112–3123 (2009)